

Author Manuscript

This is the author manuscript accepted for publication and has undergone full peer review but has not been through the copyediting, typesetting, pagination and proofreading process, which may lead to differences between this version and the [Version of Record](#). Please cite this article as [doi: 10.1111/joa.13088](https://doi.org/10.1111/joa.13088)

This article is protected by copyright. All rights reserved

1
2
3
4
5
6
7
8
9
10
11
12
13
14
15
16
17
18
19
20
21
22
23

DR. GIOVANNI BIANUCCI (Orcid ID : 0000-0001-7105-0863)

Article type : Original Paper

Corresponding Author Email ID: bianucci@dst.unipi.it

Reduction of olfactory and respiratory turbinates in the transition of whales from land to sea: the semiaquatic middle Eocene *Aegyptocetus tarfa*

Emanuele Peri¹, Philip D. Gingerich², Giacomo Aringhieri³, Giovanni Bianucci^{1*}

¹Dipartimento di Scienze della Terra, Università di Pisa, Pisa 56126, Italy

²Museum of Paleontology, University of Michigan, Ann Arbor, Michigan, 48108-2228, U.S.A

³Diagnostic and Interventional Radiology, Department of Translational Research and New Technologies in Medicine and Surgery, University of Pisa, Pisa 56126, Italy

*Corresponding author

running page heading: Turbinates of *Aegyptocetus tarfa*

24 **Abstract**

25 Ethmoturbinates, nasoturbinates, and maxilloturbinates are well developed in the narial tract of
26 land-dwelling artiodactyls ancestral to whales, but these are greatly reduced or lost entirely in
27 modern whales. *Aegyptocetus tarfa* is a semiaquatic protocetid from the middle Eocene of
28 Egypt. CT-scans of the skull show that *A. tarfa* retained all three sets of turbinates like a land
29 mammal. It is intermediate between terrestrial artiodactyls and aquatic whales in reduction of the
30 turbinates. Ethmoturbinates in *A. tarfa* have 26% of the surface area expected for an artiodactyl.
31 These have an olfactory function and indicate that early whales retained a sense of smell in the
32 transition from land to sea. Maxilloturbinates in *A. tarfa* have 6% of the surface area expected
33 for an artiodactyl. These have a respiratory function and their markedly reduced size suggests
34 that rapid inhalation and exhalation was already more important compared to warming and
35 humidifying air, in contrast with extant land mammals. Finally, the maxilloturbinates of *A. tarfa*,
36 although greatly reduced, still show some degree of similarity to those of artiodactyls, supporting
37 the phylogenetic affinity of cetaceans and artiodactyls based on morphological and molecular
38 evidence.

39

40

41

42

43 **Keywords:** Archaeoceti, Protocetidae, Artiodactyla, Eocene, turbinates, CT-scans.

44

45

46

47 **Introduction**

48 The nasal chamber of mammals typically contains three sets of epithelium-covered bony plates
49 or turbinates. Posterior turbinates associated with the ethmoid bones, the ethmoturbinates, have
50 an olfactory function (Van Valkenburgh et al. 2004, 2011; Pihlström, 2008). Anterior turbinates
51 associated with the maxillary bones, the maxilloturbinates, have a respiratory function: they
52 warm and humidify air as it is inspired, and recover heat and water from air as it is expired
53 (Hillenius, 1992, 1994; Van Valkenburgh et al. 2004; Crompton et al. 2015). Dorsal turbinates
54 associated with the nasal bones, the nasoturbinates, are located more centrally in the nasal cavity,
55 above and behind the maxilloturbinates and above and in front of the ethmoturbinates. The
56 function of the nasoturbinates is not fully understood although it seems that they have a
57 predominantly olfactory function (Hillenius, 1982; Van Valkenburgh et al. 2004, 2011; Harkema
58 et al. 2006).

59 Turbinates are present and important in almost all mammalian groups, but extant aquatic Cetacea
60 are an exception. Modern odontocetes have no turbinates at all and modern mysticetes preserve
61 only rudimentary ethmoturbinates (Godfrey et al. 2012; Godfrey 2013; Berta et al. 2014; Buono
62 et al. 2015). The fossil record shows that whales evolved from terrestrial Artiodactyla
63 (Gingerich et al. 2001; Thewissen et al. 2007; Uhen, 2010) and several genomic studies identify
64 Hippopotamidae as the closest extant relatives of cetaceans (Geisler & Theodor, 2009; Zhou et
65 al. 2011; Hassanin et al. 2012). Gatesy et al. (2013) analysed molecular and paleontological data
66 and reinforced previous molecular studies by recognising Hippopotamus within Artiodactyla as
67 the extant sister group of whales. Artiodactyls all have the three sets of turbinates, ethmoid,
68 nasal, and maxillary, well developed (Hillenius, 1992; Clifford & Witmer, 2004a, 2004b), and

69 turbinates were clearly reduced and lost as whales evolved to become fully aquatic (Berta et al.
70 2014).

71 Although the turbinates are thin, delicate bone structures that lie within the nasal cavity of a
72 skull, making them difficult to see, they are preserved in some Eocene archaeocetes, the stem
73 group for cetaceans. The first description of turbinates in an archaeocete was by Stromer
74 (Stromer, 1903) in the late Eocene basilosaurid *Saghacetus osiris*. Ethmoturbinates are
75 preserved in Stromer's specimen as delicate laminae of bone encased in fine sediment filling the
76 nasal capsule. Uhen (2004) observed similarly preserved ethmoturbinates forming a bony
77 labyrinth in another late Eocene basilosaurid, *Dorudon atrox*, where the ethmoturbinates extend
78 as far anteriorly as the mesethmoid supporting them. Ethmoturbinates were identified in a
79 specimen attributed to the middle Eocene remingtonocetid *Andrewsiphium* sp. (Pihlström, 2008;
80 Thewissen & Nummela, 2008), and a ridge for possible attachment of maxilloturbinates was
81 identified in *Remingtonocetus* (Bajpai et al. 2011). Ethmoturbinates have also been reported in
82 the middle Eocene protocetids *Artiocetus clavis* (Fahlke et al. 2011), *Aegyptocetus tarfa*
83 (Bianucci & Gingerich, 2011), and a protocetid of unknown genus and species (Godfrey et al.
84 2012). Neither nasoturbinates nor maxilloturbinates were observed in these specimens.

85 The purpose of this study is to reconstruct the three-dimensional size and shape of turbinates in
86 the nasal cavity of the holotype of *Aegyptocetus tarfa*, and to comment on their function and
87 stage of reduction relative to artiodactyls as land mammals and to extant cetaceans as fully
88 aquatic mammals. The holotype of *A. tarfa* is exceptionally well preserved. It was found in fine-
89 grained marbleized limestone from the middle Eocene of Egypt after it was exported
90 commercially to Italy, where the limestone was cut into slabs of decorative facing stone,
91 revealing the fossil. The specimen, a partial skeleton, is preserved in the Museo di Storia

92 Naturale dell'Università di Pisa (MSNUP). Bianucci and Gingerich (2011) described
93 ethmoturbinates visible on the surface of one of the limestone slabs. Here we use Computerized
94 Axial Tomography (CT) to study the full set of turbinates in *A. tarfa*. Nasoturbinates and
95 maxilloturbinates are present in *A. tarfa* in addition to ethmoturbinates, which enables the first
96 quantitative description of turbinate surface areas within an archaeocete and the first quantitative
97 comparison with artiodactyls as representatives of the land-mammal ancestry of whales.

98

99 **Materials and methods**

100 We analysed the skull of the holotype of *Aegyptocetus tarfa* (MSNUP I15459) and, for
101 comparison, skulls of the following five extant artiodactyls in the zoological collections of the
102 MSNUP:

- 103 • *Alcelaphus buselaphus buselaphus* (Bovidae: African hartebeest) (MSNUP C1343)
- 104 • *Boselaphus tragocamelus* (Bovidae: Indian nilgai) (MSNUP C1423)
- 105 • *Camelus dromedarius* (Camelidae: Arabian camel) (MSNUP C1435)
- 106 • *Hippopotamus amphibius* (Hippopotamidae: African hippopotamus) (MSNUP C228)
- 107 • *Sus scrofa* (Suidae: Eurasian wild pig) (MSNUP C1418)

108

109 Specimens were chosen to represent a range of shape and size variation from turbinates in skulls
110 of artiodactyls comparable in size to *A. tarfa*. All skulls were CT-scanned in Azienda
111 Ospedaliero-Universitaria di Pisa. The machine used was a GE LightSpeed RT 16, with a slice
112 thickness of 1.25 mm and spacing between slices of 0.625 mm. CT-scans were analysed with
113 open-access Mango software for medical image visualization (Multi-image Analysis GUI;
114 <http://rii.uthscsa.edu/mango/>). Mango was also used to create virtual 3D models of turbinates

115 and to calculate their surface area. The skull of *A. tarfa* is weakly asymmetrical due to its
116 clockwise torsion (Bianucci & Gingerich, 2011), so turbinates were mapped on both sides.
117 Artiodactyl skulls are bilaterally symmetrical, and mapping was confined to turbinates of the left
118 side of the skull (Ranslow et al. 2014). Surface area measurements for artiodactyls were then
119 doubled to represent both left and right sides.

120 There are two sources of uncertainty in measurements of the fossil *A. tarfa*. Differences in bone
121 and sediment density enabled reconstruction of the three-dimensional shape of turbinates when
122 surrounded by calcareous matrix, but the resolution was lower than for skulls of extant
123 artiodactyls with empty nasal cavities. In addition, it was necessary to reconstruct turbinates
124 damaged when the *A. tarfa* skull entombed in matrix was cut into slabs (Bianucci & Gingerich,
125 2011). Uncertainty of measurements in the extant artiodactyls was due to breakage of the
126 thinnest laminae of bone. All these sources of uncertainty cause turbinate areas to be similarly
127 underestimated, meaning comparisons should still be reliable within and between taxa.

128 The relative sizes of turbinates in *A. tarfa* were compared to those of artiodactyls in three ways.
129 First, we compared the area of the ethmoturbinate surface (ETS), the area of the nasoturbinate
130 surface (NTS), and the area of the maxilloturbinate surface (MTS), to the total turbinate surface
131 (TTS). In the second comparison we measured the size of the turbinate chamber surface (TCS)
132 within the nasal chamber of *A. tarfa*. This measured value of TCS was then compared to TCS
133 for an animal the skull length, bizygomatic skull width, and body weight of *A. tarfa*, based on
134 TCS measured in the five extant artiodactyls. Turbinates do not fill the whole nasal chamber.
135 The anterior end of the turbinate chamber coincides with the anterior extremity of the
136 maxilloturbinates, and its posterior end coincides with the ethmoidal portion of the cribriform
137 plate (excluding the maxilla). In this comparison the natural logarithm (\ln) of the square root of

138 TCS was regressed on ln cranial length (cm), on ln cranial width (cm), and on ln cube root of
139 body weight (kg) for the artiodactyls. TCS was measured using the same methods as those
140 described above for calculating the surface area of turbinates. Skull length and width were
141 measured on the skulls used for CT-scanning. The body weight for *A. tarfa* is that estimated by
142 Bianucci & Gingerich (2011). Body weights for the artiodactyls were estimated from a
143 regression of body weight on skull length (Janis, 1990).
144 Finally, we compared the surface area for each set of turbinates, ETS, NTS, and MTS, to the area
145 expected, based on extant artiodactyl, for the set given the associated TCS. Measured values for
146 ETS, NTS, and MTS in *A. tarfa* were compared to the values expected from regressions of
147 artiodactyl ETS, NTS, and MTS on TCS.

148 **Results**

149 CT-scans show that the turbinate sets in Eocene *A. tarfa* are slightly asymmetrical (Fig. 1A,B).
150 This feature is possibly related to the clockwise torsion of the rostrum (Bianucci & Gingerich,
151 2011), a genuine anatomical feature that has also been observed in other archaeocetes (Fahlke et al.
152 2011; Fahlke and Hampe, 2015). This hypothesis is supported by the fact that, in *A. tarfa*, the
153 maxilloturbinates, which extend more anteriorly in the rostrum than ethmoturbinates and
154 nasoturbinates, exhibit the greater degree of asymmetry (i.e., the right maxilloturbinates are
155 slightly wider transversely than the left maxilloturbinates). The ethmoturbinates, like those in
156 other mammals (Hillenius, 1994), are convoluted and densely packed in the olfactory recess.
157 Left and right nasoturbinates are elongated, narrow, and, for most of their length, a single
158 laterally-concave lamina of bone. Posteriorly a second medially-concave plate appears, giving
159 the nasoturbinates in this region a more tubular appearance. Left and right maxilloturbinates are
160 small compared to those of modern artiodactyls (Fig. 1C–H), and the maxilloturbinates occupy a

161 relatively small portion of the nasal chamber. They do not extend anteriorly beyond the
162 nasoturbinates. Their morphology is simple: the most anterior part of the lamina is hook-shaped
163 and concave dorsally and laterally (Fig. 2A). There is a narrow downward-facing lamina in the
164 middle part, and the posterior part of the lamina is again hook-shaped.

165 Maxilloturbinates of *A. tarfa* and the five artiodactyls studied for comparison are illustrated in
166 red in the cross sections of skulls in Fig. 2. All of the artiodactyls have elongated, double (lower
167 and upper) scroll-shaped maxilloturbinates without projecting branches (Fig. 2B–F). The upper
168 scroll is more developed and convoluted than the lower scroll. These features, which have been
169 observed in all specimens, are typical of and exclusive to artiodactyls (Hillenius, 1992). For
170 example, the maxilloturbinates of *Equus caballus* (Perissodactyla) have a single high and narrow
171 scroll; also, they show a greater thickness than the maxilloturbinates of artiodactyls (Arencibia et
172 al. 2000: figures 7–8, where the maxilloturbinates are named “ventral conchal bulla”). Carnivora
173 have richly-branching double-scroll-shaped maxilloturbinates (Van Vakenburgh et al. 2004).

174 The maxilloturbinates of *A. tarfa* clearly differ from those of carnivores in lacking the external
175 branches, while they exhibit some affinities with those of artiodactyls. Indeed, the
176 maxilloturbinates of *A. tarfa* could be considered a simplified version of the artiodactyl double
177 scroll (Fig. 2A). The upper scroll in *A. tarfa* is reduced to only one half-round. The lower scroll
178 has almost disappeared but there is a small branch at mid-length of the maxilloturbinates
179 suggesting a lower scroll. Similarities to *Equus caballus* are weaker because the latter has the
180 lower scroll completely missing (Arencibia et al. 2000).

181 Measurements for each set of turbinates are given in Table 1. When we compare the ETS, NTS,
182 and MTS areas for artiodactyls to their sum, TTS, we find modal proportions of 0.42, 0.14, and
183 0.41, respectively. These proportions are 0.61, 0.20, and 0.15 in *A. tarfa*, indicating that *A. tarfa*

184 has more of its turbinate area devoted to ethmoturbinates than expected from comparison to
185 artiodactyls, and less devoted to maxilloturbinates.

186 We can compare turbinate size in a different way by asking how the area of TCS compares to
187 body size measured by skull length, skull width, or body weight. *A. tarfa* has a skull length of 68
188 cm (table 1). Regression of $\ln \sqrt{\text{TCS}}$ on skull length for artiodactyls (Fig. 3A) yields an
189 expected TCS for *A. tarfa* of 195604 mm², corresponding to \ln square-root value of about 6.092.
190 The observed TCS for *A. tarfa* is 64953 mm², corresponding to \ln square-root value of 5.541.
191 Thus, the residual for length (observed-minus-expected) is calculated to be -0.549 and the
192 corresponding proportion 0.333. In the previous paragraph we found that TCS of *A. tarfa* is
193 about 33% as large as expected for an artiodactyl of the same skull length.

194 Similar calculations show that TCS for *A. tarfa* is about 57% as large as expected for an
195 artiodactyl of the same skull width, and about 63% as large as expected for an artiodactyl of the
196 same body weight. Variation in the residuals and proportions observed here are probably related
197 to differences in skull shape for the species compared. Taking the median, we conclude that the
198 area of TCS is about 57% as large as expected in an artiodactyl of the same size.

199 Another way to compare turbinate size is to compare the turbinate area observed in *A. tarfa* with
200 the turbinate area expected for an artiodactyl of the same TCS. The comparison for
201 ethmoturbinates is shown in Fig. 3B, where the observed-minus-expected residual for \ln ETS is
202 -0.76, and ETS itself is 0.47 the size expected for TCS observed in *A. tarfa*. Similar calculations
203 for nasoturbinates and maxilloturbinates are shown in Fig. 3C-D, where the residuals are -0.78
204 and -2.30, respectively, and the corresponding proportions for NTS and MTS are 0.46 and 0.10
205 the size expected for TCS observed in *A. tarfa*. Combining all observations in Fig. 3 by
206 multiplying each proportion in Fig. 3b-d by 0.566 from Fig. 3A, ETS and NTS for *A. tarfa* are

207 each about 26% of the size expected for an artiodactyl, and MTS for *A. tarfa* is about 6% of the
208 size expected for an artiodactyl.

209

210

211 **Discussion**

212 **Morphofunctional considerations**

213 The general trend of reduction of turbinate size from artiodactyls to extant cetaceans (Berta et al.

214 2014) is supported by three-dimensional reconstruction of the turbinates of *A. tarfa* and

215 comparison of their size and shape to the turbinates of extant artiodactyls. Ethmoturbinates,

216 nasoturbinates, and maxilloturbinates are all retained in *A. tarfa*, but all are reduced in size

217 compared to expectation based on artiodactyls. As calculated above, ETS and NTS are each

218 about 26% of the area expected for an artiodactyl, and MTS is about 6% of the expected size.

219 This atrophy in *A. tarfa* cannot have been caused by post-mortem breakage because observations

220 made on cross sections of the skull before reassembly showed excellent preservation of the

221 turbinates (Bianucci & Gingerich, 2011: figures 4-5). Further, three-dimensional reconstruction

222 of the *A. tarfa* turbinates shows a close correspondence of turbinates on the left and right sides of

223 the skull. Thus, we consider the turbinates of *A. tarfa*, to be complete (except for the parts

224 destroyed by the cuts) and regard the reconstruction shown in Fig. 1A–B as reliable.

225 An ethmoturbinate and nasoturbinate reduction to 26% of expected value in *A. tarfa* is relatively

226 easy to explain. Terrestrial mammals use olfaction to locate food and to communicate in social

227 interactions (Hillenius, 1992, 1994; Van Valkenburgh et al. 2011). *A. tarfa* was a semiaquatic

228 predator, hunting in water like other protocetids (Gingerich, 2003; Bianucci & Gingerich, 2011).

229 Mammalian olfactory receptors differ from those of fishes and amphibians and do not work well

230 in water (Pihlström, 2012), so olfaction would have had limited use for locating prey. *A. tarfa*,

231 like other protocetids, was considered able to hear high sonic frequencies, facilitating predation
232 on sound-producing fish (Bianucci & Gingerich, 2011; Fahlke et al. 2011), although a recent
233 study based on the cochlear morphology questioned specialization for ultrasonic hearing among
234 archaeocetes (Mourlam & Orliac, 2017).

235 Reduction of ethmoturbinates is also observed in pinnipeds. Van Valkenburgh et al. (2011),
236 citing Laska (2005), interpreted ethmoturbinate reduction in pinnipeds to reflect a reduction in
237 olfactory acuity, the range of smells that can be detected, but not olfactory sensitivity or
238 discrimination within a narrower range. Based on this reasoning, *A. tarfa* was probably able to
239 detect and distinguish a restricted range of smells when on land or on the sea surface. This
240 would be important for mate identification and calf recognition.

241 Near complete atrophy of maxilloturbinates in *A. tarfa* is more difficult to explain.

242 Maxilloturbinates play an important role in heat and water retention in modern mammals. Van
243 Valkenburgh et al. (2011) found the surface area of ethmoidal or olfactory turbinates to be about
244 three times greater than the surface area of maxillary or respiratory turbinates in terrestrial
245 carnivores, and the opposite to be true in aquatic carnivores. Pinnipeds, with marine adaptations
246 paralleling those of protocetids, have maxilloturbinates with a greater surface area than their
247 ethmoturbinates (Van Valkenburgh et al. 2011), which is the opposite of what we see in
248 comparing *A. tarfa* to artiodactyls or to terrestrial carnivores (Van Valkenburgh et al. 2011).

249 Modern cetaceans have a smooth-walled narial tract lacking respiratory turbinates, which
250 Reidenberg & Laitman (2008) consider an advantage for rapid friction-free exchange of large
251 volumes of air during brief breathing events at the sea surface. Rapid transfer of air during
252 breathing may have been important for protocetids like *A. tarfa*. Middle Eocene oceans were 6–
253 8 °C warmer than oceans today (Zachos, 2001) and the relatively constant humidity of an

254 evaporative environment at the sea surface would reduce the need for both heat and water
255 retention. The extreme reduction of maxilloturbinates could also be a consequence of the
256 moderate posterior shift of the position of the external bony nares observed in *A. tarfa* and other
257 protocetids. In fact, such a shift reduced the length of the nasal passage. The retention of reduced
258 turbinates in some archaic odontocetes displaying limited telescoping and external bony nares that
259 still do not reach the vertex of the skull (Churchill et al. 2018) lends some support to this
260 hypothesis.

261

262 **Phylogenetic considerations**

263 The comparison of turbinate cross sections in Fig. 2 shows that maxilloturbinates of *A. tarfa*,
264 although greatly reduced, still show some similarity to those of artiodactyls, supporting the
265 phylogenetic affinity of cetaceans and artiodactyls based on other evidence (Gingerich et al.
266 2001; Thewissen et al. 2007; Uhen, 2010). Morphological differences between the
267 maxilloturbinates of cetaceans and artiodactyls (both having the typical double scroll
268 morphology) compared to perissodactyls (with only an upper scroll) and carnivores (where
269 branching turbinates replace scrolls) are consistent with the phylogenetic distance between these
270 three mammalian clades.

271 Molecular analyses place Hippopotamidae, within extant Artiodactyla, as the closest living
272 relative of Cetacea (Geisler & Theodor, 2009; Zhou et al. 2011; Hassanin et al. 2012; Gatesy et
273 al. 2013), with the divergence time of hippos and cetaceans estimated at 52.4 Ma (Orliac et al.
274 2010). Maxilloturbinates of *Hippopotamus amphibius* are most similar to those of other
275 artiodactyls and do not show any special similarity to maxilloturbinates of *A. tarfa* (Fig. 2). This
276 is not surprising considering the great reduction of maxilloturbinates in *A. tarfa*.

277

278 **Acknowledgments**

279 We thank Simone Farina and Chiara Sorbini for providing access to collections under their care,
280 Davide Caramella and Davide Giustini for the CT scanning and for useful suggestions about the
281 processing of CT-scan images, and Walter Landini for stimulating discussions.

282
283 **Author contributions**

284 EP and GA analysed and processed the CT-scan images, EP, GB, and PDG, wrote the paper, GB
285 supervised the project, all authors discussed the paper and gave the final approval for
286 publication.

287
288 **Competing interests**

289 We declare we have no competing interests.

290
291 **References**

- 292
293 **Arencibia A, Vazquez JM, Jaber R, et al.** (2000) Magnetic resonance imaging and cross
294 sectional anatomy of the normal equine sinuses and nasal passages. *Veter Radiol Ultras* **41**,
295 313–319.
- 296 **Bajpai S, Thewissen JGM, Conley RW** (2011) Cranial anatomy of middle Eocene
297 *Remingtonocetus* (Cetacea, Mammalia) from Kutch, India. *J Paleont* **85**, 703–718.
- 298 **Berta A, Ekdale EG, Cranford TW** (2014) Review of the Cetacean Nose: Form, Function, and
299 Evolution. *Anat Rec* **297**, 2205–2215.

- 300 **Buono MR, Fernández MS, Fordyce RE, Reidenberg J S** (2015) Anatomy of nasal complex
301 in the southern right whale, *Eubalaena australis* (Cetacea, Mysticeti). *J. Anatomy* **226**, 80-92.
- 302 **Bianucci G, Gingerich PD** (2011) *Aegyptocetus tarfa*, n. gen. et sp. (Mammalia, Cetacea), from
303 the middle Eocene of Egypt: clinorhynch, olfaction, and hearing in a protocetid whale. *J Vert*
304 *Paleont* **31**, 1173–1188.
- 305 **Clifford AB, Witmer LM** (2004a) Case studies in novel narial anatomy: 2. The enigmatic nose
306 of moose (Artiodactyla: Cervidae: *Alces alces*). *J Zool* **262**, 339–360.
- 307 **Clifford AB, Witmer LM** (2004b) Case studies in novel narial anatomy: 3. Structure and
308 function of the nasal cavity of saiga (Artiodactyla: Bovidae: *Saiga tatarica*). *J Zool* **264**, 217–
309 230.
- 310 **Crompton AW, Musinsky C, Owerkowicz T** (2015) Evolution of the mammalian nose. In
311 *Great Transformations in Vertebrate Evolution*. (ed. Dial K, Shubin N, Brainerd E), pp. 189–
312 203. Chicago, IL: University of Chicago Press.
- 313 **Churchill M, Geisler JH, Beatty BL, Goswami A** (2018) Evolution of cranial telescoping in
314 echolocating whales (Cetacea: Odontoceti). *Evolution* **72**, 1092-1108.
- 315 **Fahlke JM, Gingerich PD, Welsh RC, Wood AR** (2011) Cranial asymmetry in Eocene
316 archaeocete whales and the evolution of directional hearing in water. *PNAS* **108**, 14545–
317 14548.
- 318 **Fahlke JM, Hampe O** (2015) Cranial symmetry in baleen whales (Cetacea, Mysticeti) and the
319 occurrence of cranial asymmetry throughout cetacean evolution. *Sci Nat*, **102**, 1-16.
- 320 **Gatesy J, Geisler JH, Chang J, et al.** (2013) A phylogenetic blueprint for a modern whale. *Mol*
321 *Phylogenet Evol* **66**, 479–506.
- 322 **Geisler JH, Theodor JM** (2009) Hippopotamus and whale phylogeny. *Nature* **458**, E1–E4.

323 **Gingerich PD** (2003) Land-to-sea transition in early whales: evolution of Eocene Archaeoceti
324 (Cetacea) in relation to skeletal proportions and locomotion of living semiaquatic mammals.
325 *Paleobiology* **29**, 429–454.

326 **Gingerich PD, ul Haq M, Zalmout IS, Khan IH, Malkani MS** (2001) Origin of Whales from
327 Early Artiodactyls: Hands and Feet of Eocene Protocetidae from Pakistan. *Science* **293**, 2239–
328 2242.

329 **Godfrey SJ** (2013) On the olfactory apparatus in the Miocene odontocete *Squalodon* sp.
330 (*Squalodontidae*). *C R Palevol* **12**, 519–530.

331 **Godfrey SJ, Geisler J, Fitzgerald EMG** (2012) On the olfactory anatomy in an archaic whale
332 (*Protocetidae*, Cetacea) and the minke whale *Balaenoptera acutorostrata* (*Balaenopteridae*,
333 Cetacea). *Anat Rec* **296**, 257–272.

334 **Harkema JR, Carey SA, Wagner JG** (2006) The nose revisited: a brief review of the
335 comparative structure, function, and toxicologic pathology of the nasal epithelium. *Toxicol*
336 *Pathol* **34**, 252–269.

337 **Hassanin A, Delsuc F, Ropiquet A, et al.** (2012) Pattern and timing of diversification of
338 Cetartiodactyla (Mammalia, Laurasiatheria), as revealed by a comprehensive analysis of
339 mitochondrial genomes. *C R Biol* **335**, 32–50.

340 **Hillenius WJ** (1992) The evolution of nasal turbinates and mammalian endothermy.
341 *Paleobiology* **18**, 17-29.

342 **Hillenius WJ** (1994) Turbinates in therapsids: evidence for late Permian origins of mammalian
343 endothermy. *Evolution* **48**, 207-229.

344 **Janis CM** (1990) Correlation of cranial and dental variables with dietary preferences in
345 mammals: a comparison of macropodoids and ungulates. *Mem Queensland Mus* **28**, 349-366.

346 **Laska M** (2005) the number of functional olfactory receptor genes and the relative size of
347 olfactory brain structures are poor predictors of olfactory discrimination performance with
348 enantiomers. *Chem Senses* **30**, 171–175.

349 **Mourlam MJ, Orliac MJ** (2017) Infrasonic and ultrasonic hearing evolved after the emergence
350 of modern whales. *Curr Biol* **27**, 1776-1781.

351 **Orliac M, Boisserie J-R, MacLatchy L, Lihoreau F** (2010) Early Miocene hippopotamids
352 (Cetartiodactyla) constrain the phylogenetic and spatiotemporal settings of hippopotamid
353 origin. *PNAS* **107**, 11871–11876.

354 **Pihlström H** (2008) Comparative anatomy and physiology of chemical senses in aquatic
355 mammals. In *Sensory evolution on the threshold: Adaptations in Secondarily Aquatic*
356 *Vertebrates* (ed Thewissen JGM, Nummela S) pp. 95–109. Berkeley, CA: University of
357 California Press.

358 **Pihlström H** (2012) The size of major mammalian sensory organs as measured from cranial
359 characters, and their relation to the biology and evolution of mammals. *Dissertationes*
360 *Biocentri Viikki Universitatis Helsingiensis* **44**.

361 **Ranslow AN, Richter JP, Neuberger T, et al.** (2014) Reconstruction and morphometric
362 analysis of the nasal airway of the white-tailed deer (*Odocoileus virginianus*) and implications
363 regarding respiratory and olfactory airflow. *Anat Rec* **297**, 2138–2147.

364 **Reidenberg JS, Laitman JT** (2008) Sisters of the sinuses: cetacean air sacs. *Anat Rec* **291**,
365 1389–1396.

366 **Stromer E** (1903) Zeuglodon-reste aus dem Oberen Mittellocän des Fajum. *Beitr Paläont*
367 *Österreich-Ungarns Orients* **15**, 65–100.

368 **Thewissen JGM, Cooper LN, Clementz MT, Bajpai S, Tiwari BN** (2007) Whales originated
369 from aquatic artiodactyls in the Eocene epoch of India. *Nature* **450**, 1190–1194.

370 **Thewissen JGM, Nummela S** (2008) Sensory evolution in aquatic tetrapods: toward and
371 integrative approach. In *Sensory evolution on the threshold: Adaptations in Secondarily*
372 *Aquatic Vertebrates* (ed Thewissen JGM, Nummela S) pp. pp. 333–340. Berkeley, CA:
373 University of California Press.

374 **Uhen MD** (2004) Form, function, and anatomy of *Dorudon atrox* (Mammalia, Cetacea): an
375 Archaeocete from the Middle to Late Eocene of Egypt. *Univ Michigan Paleont Papers* **34**, 1–
376 222.

377 **Uhen MD** (2010) The Origin(s) of Whales. *Annu Rev Earth Planet Sci* **38**, 189–219.

378 **Van Valkenburgh B, Curtis A, Samuels JX, et al.** (2011) Aquatic adaptations in the nose of
379 carnivorans: evidence from the turbinates. *J Anatomy* **218**, 298–310.

380 **Van Valkenburgh B, Theodor J, Friscia A, Pollack A, Rowe T** (2004) Respiratory turbinates
381 of canids and felids: a quantitative comparison. *J Zool* **264**, 281–293.

382 **Zachos J** (2001) Trends, rhythms, and aberrations in global climate 65 Ma to Present. *Science*
383 **292**, 686–693.

384 **Zhou X, Xu S, Yang Y, Zhou K, Yang G** (2011) Phylogenomic analyses and improved
385 resolution of Cetartiodactyla. *Mol Phylogenet Evol* **61**, 255–264.

386

Figure captions

387

388

389 **Figure 1** Three-dimensional CT-scan reconstruction of skulls and related turbinates in dorsal and
390 lateral view. (A,B) *Aegyptocetus tarfa*, MSNUP I15459. (C,D) *Alcelaphus buselaphus*, MSNUP
391 C1343. (E,F) *Camelus dromedarius*, MSNUP C1435. (G,H) *Boselaphus tragocamelus*,
392 MSNUP C1423. Scale bar is 10 cm.

393

394 **Figure 2** Left and right maxilloturbinates (red) and nasoturbinates (blue) in CT-scan cross
395 sections of skulls studied here. (A) *Aegyptocetus tarfa*, MSNUP I15459. (B) *Alcelaphus*
396 *buselaphus*, MSNUP C1343. (C) *Sus scrofa*, MSNUP C1418. (D) *Hippopotamus amphibious*,
397 MSNUP C228. (E) *Camelus dromedarius*, MSNUP C1435. (F) *Boselaphus tragocamelus*,
398 MSNUP C1423. All sections were taken at the anteroposterior midpoint of the maxilloturbinates
399 and all sections are reduced to the same height. Note the small size and simple structure of
400 maxilloturbinates in *A. tarfa* compared to those of artiodactyls.

401

402 **Figure 3** Turbinate size observed in middle Eocene *Aegyptocetus tarfa* (solid symbols)
403 compared to turbinate size in five species of extant artiodactyls (open symbols). (A) allometric
404 scaling of TCS with length, width, and the cube-root of body weight. (B) allometric scaling of
405 ETS with TCS. (C) allometric scaling of NTS with TCS. (D) allometric scaling of MTS with
406 TCS. Dashed lines are projections showing the distance between observation and expectation.
407 ‘Proportion’ is the residual expressed as a ratio of observation to expectation. ‘Combined’ is the
408 median proportion in (A) multiplied by the proportion in (B), (C), or (D). Measurements plotted
409 here are listed in Table 1. (Online version in colour.)

410

411

412

413

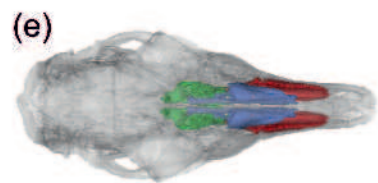
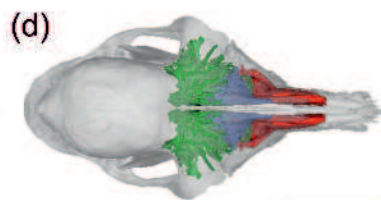
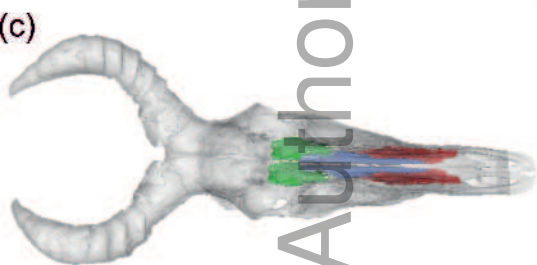
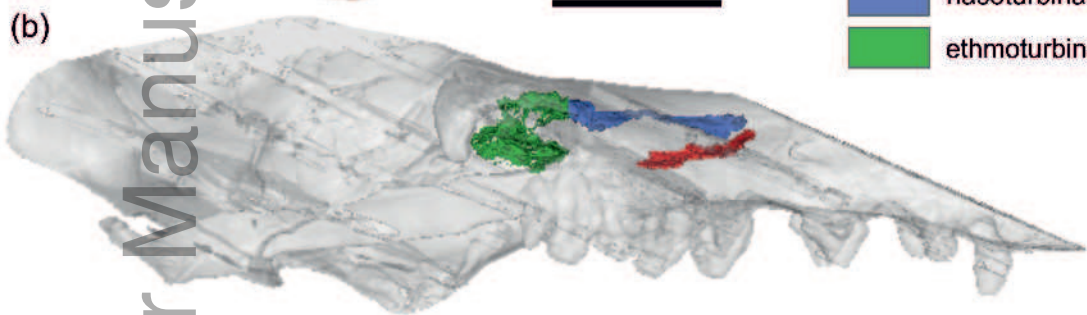
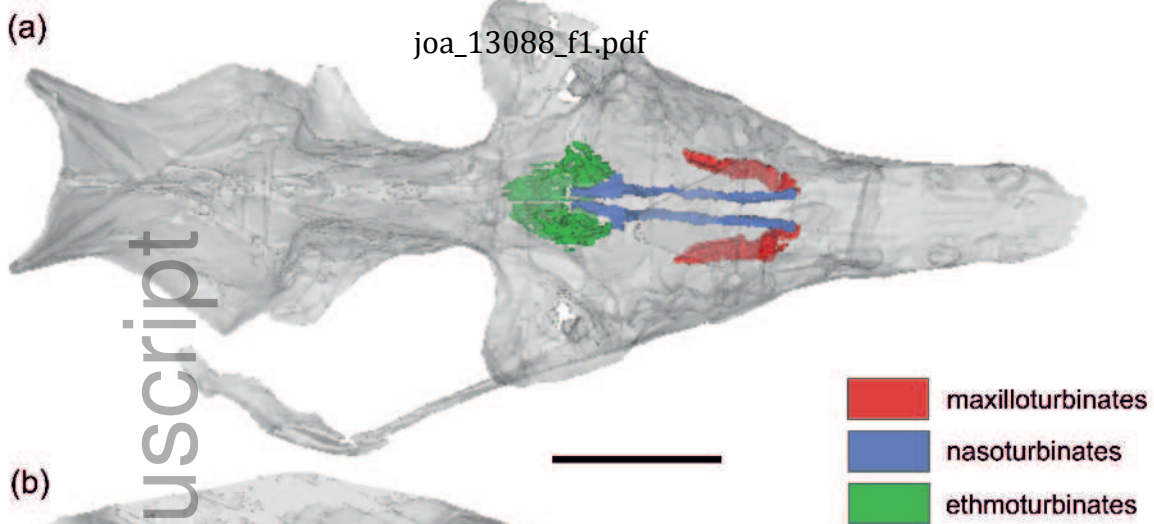
414 **Table 1** Measurements of body size, turbinate chamber surface area, and ethmoturbinate,
 415 nasoturbinate, and maxilloturbinate surface areas in comparative Artiodactyla and the middle
 416 Eocene archaeocete *Aegyptocetus tarfa*. Right-hand columns list ETS, NTS, and MTS as a
 417 proportion of TTS. Medians are in bold-face type.

Genus and species	Cranial length (cm)	Cranial width (cm)	Body weight (kg)	TCS (mm ²)	ETS (mm ²)	NTS (mm ²)	MTS (mm ²)	TTS (mm ²)	ETS/TTS	NTS/TTS	MTS/TTS
ARTIODACTYLA											
<i>Boselphus tragocamelus</i>	38.0	15.4	227	63813	25262	12532	53745	91540	0.28	0.14	0.59
<i>Alcelaphus buselaphus</i>	34.6	11.5	309	63355	30424	19355	44117	93896	0.32	0.21	0.47
<i>Hippopotamus amphibius</i>	63.6	37.4	1532	177606	114138	32039	102397	248574	0.46	0.13	0.41
<i>Camelus dromedarius</i>	34.0	15.0	260	51298	55753	11232	42677	109662	0.51	0.10	0.39
<i>Sus scrofa</i>	30.9	15.6	122	52376	22274	11011	19513	52798	0.42	0.21	0.37
Medians:	34.6	15.4	260	63355	30424	12532	44117	93896	0.42	0.14	0.41
ARCHAEOCETI											
<i>Aegyptocetus tarfa</i>	68.0	27.0	650	64953	17010	6638	4158	27806	0.61	0.24	0.15

418

419

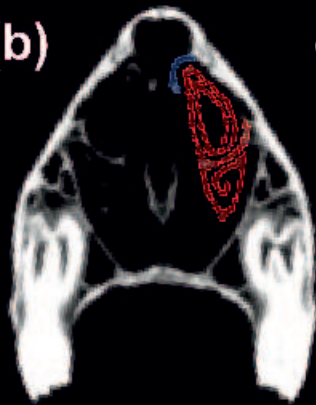
420



(a)



(b)



(c)



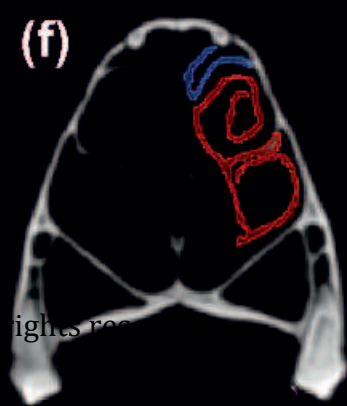
(d)



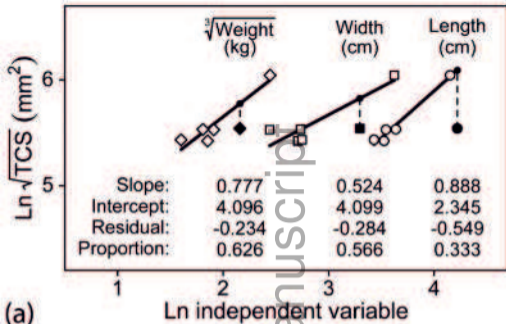
(e)



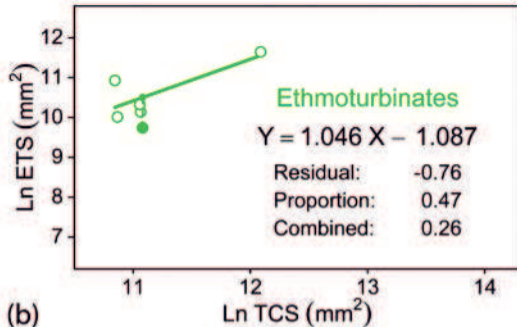
(f)



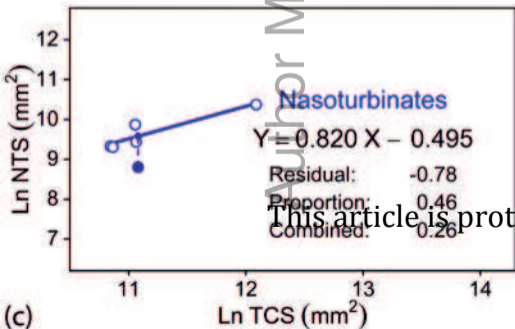
This article is protected by copyright. All rights reserved.



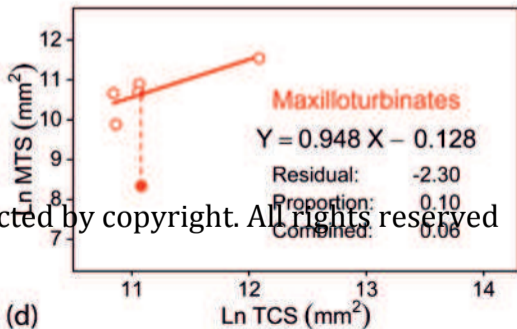
(a)



(b)



(c)



(d)

This article is protected by copyright. All rights reserved